An Evaluation of the Effect of Prepulses on HF Laser-Target Interactions

M. Keith Matzen

SAND79-0353
Unlimited Release
Printed June 1979

AN EVALUATION OF THE EFFECT OF PREPULSES ON HF LASER-TARGET INTERACTIONS

M. Keith Matzen
Division 4211
Sandia Laboratories, Albuquerque, NM 87185

ABSTRACT

We have assessed the effect of multinanosecond, low-power-density prepulses on the interaction of multinanosecond, 10^{14} W/cm^2, ~ 3 μm HF laser pulses with slab targets. The emphasis is on analyzing absorption and x-ray conversion efficiency. A survey of previous experiments gives no evidence that these prepulses will affect the total absorption. However, prepulses have been observed to cause qualitative changes in both the x-ray spectrum and conversion efficiency. Numerical simulations indicate that the laser-target interaction is effectively insensitive to low-power-density prepulses. These studies imply that basic laser-target experiments with multiplexed, HF laser pulses will provide an important characterization of the interaction of long pulse, multi-line, ~ 3 μm radiation with targets. Future wavelength comparison experiments will require prepulse suppression or target isolation.

TABLE OF CONTENTS

I. Introduction

The PHOENIX II HF amplifier system which is under development at Sandia Laboratories will have the capability to deliver approximately 1 kJ in a 50 ns pulse. To obtain shorter pulses (5-10 ns) of interest to both weapons-effects-simulation and laser-fusion applications, a multiple beam extraction scheme (angular multiplexing) will be used. The oscillator pulses[1] which will be used in this scheme presently have a long prepulse immediately preceding the main pulse. If the contrast ratio of the oscillator pulse is maintained throughout the amplifier chain, a multinanosecond pulse extracted from the PHOENIX II amplifier will be preceded by a multinanosecond prepulse with a contrast ratio of 10^2. In order to determine experimental priorities, we must decide if meaningful laser-target experiments can be performed with the expected, 10^2-contrast-ratio pulses. Therefore, in this report we assess the importance of this type of prepulse on the following aspects of laser-target interactions:

absorption and stimulated scattering,

hot electron production,

x-ray conversion efficiency,

x-ray spectrum,

target ablation, and

thermal conductivity.

Of course, all of these areas are not independent, but in general, they represent the areas of concentration of both previous laser-target experiments and the the initial HF laser-target experiments. We will emphasize absorption and x-ray conversion efficiency studies in this report. Although the goals of the laser-fusion and the weapons-effects-simulation programs are different an understanding of the effect of a prepulse on the above areas is important for both programs.

We will first present a general discussion of prepulses and a qualitative assessment of their importance in ICF laser-target experiments. Next, we will summarize the previous experiments on prepulse effects and infer that the experimental results are inconclusive, particularly for long pulses. Finally, we will discuss a set of computer simulations which indicate that a contrast ratio of 10^2 should not significantly affect long-pulse, laser-target interactions.

II. Overview of Prepulse Effects

A consideration of the prepulse is important because the prepulse can form a plasma at the target surface which alters the interaction of the main pulse with the target. The prepulse can occur in many forms: the long time ($\gtrsim \mu$s) ASE occurring in the laser chain before the main pulse, a slow rise time of the main pulse itself, a distinct pulse amplified through the chain before the main pulse, or a leading "foot" of relatively short time duration ($\sim$ few ns) which immediately precedes the main pulse. The nature and power density of prepulses have been important considerations in previous laser-fusion studies because the emphasis has been on neutron production from exploding-pusher targets. Exploding pusher targets require subnanosecond pulses with a fast rise time; the plasma produced by a prepulse degrades the target performance. Experiments at LASL[2] have shown that the prepulse power density must be less than $\sim 10^9$ W/cm^2 to avoid plasma production. Work with long, 1.06-μm pulses at NRL[3] confirms this intensity threshold; interferometric measurements show that plasma formation begins approximately 8 ns before the peak of a roughly Gaussian, 3-ns (FWHM) pulse, that is, at a power density of approximately 10^9 W/cm^2. Plasma formation has been observed[4] at power densities as low as $\sim 10^8$ W/cm^2. Although the prepulse must be kept below this threshold for exploding pusher targets and the current, subnanosecond-type, complex laser-fusion targets, the importance of a prepulse on ablatively-driven or reactor-type laser-fusion targets and weapons-effects-simulation targets has not been assessed. For the multinanosecond laser pulses proposed for future experiments, effects of the plasma produced by any low-power-density prepulse may be insignificant compared to the effects of the plasma produced during the early time of the main pulse. As the NRL experiments[3] have shown, the slow rise time of these long pulses can also give rise to significant plasma formation. Furthermore, many ablative-

target designs require a shaped pulse with a moderate power density foot in order to enhance the compression.[5] Thus, it is not clear that the proposed, multiplexed, HF laser pulses with a main pulse of 5 to 20 ns and a leading-foot prepulse of equal time duration will have any negative features for future laser-fusion or weapons-effects-simulation target studies.

III. Effect of a Prepulse on Absorption and Scattering

Several laboratories have performed experiments to determine the effect of a prepulse on laser-target interactions. The more recent studies at NRL[6-10] and Ecole Polytechnique[11] emphasized absorption and backscatter measurements while the earlier experiments at Battelle[12] emphasized x-ray conversion efficiencies. NRL's work is the most extensive; they varied the pulse length from 21 ps to 900 ps, the time between prepulse and main pulse from 700 ps to 2 ns, the ratio of the energy in the prepulse to the total incident energy from 10^{-4} to 0.2, and the main pulse power density on target from 10^{13} W/cm^2 to 10^{16} W/cm^2. Because these prepulses consist of a distinct pulse rather than a leading foot, and because these pulse lengths are considerably shorter than our multinanosecond HF pulses, the applicability of their results to proposed HF experiments is questionable. Nevertheless, several conclusions are worth mentioning. First, the backscattered radiation is attributed to the Brillouin backscatter instability, with other scattering mechanisms believed to be insignificant.[8-10] Second, the threshold for backscatter appears to be in the neighborhood of 10^{13} W/cm^2.(8) Third, although no parameters were varied consistently over the entire 10^{13} - 10^{16} W/cm^2 range, the backscatter appears to increase with increasing power density when prepulses are present. For example, the fraction of laser energy backscattered was approximately 1% and 5% (900-ps FWHM) at 10^{13} W/cm^2 and 10^{14} W/cm^2,(3,10) respectively, greater than 10% at 10^{15} W/cm^2, and as much as 50% at 10^{16} W/cm^2 (75-ps FWHM).[8,9] Obviously, this

increased backscatter can significantly decrease the absorption of these subnanosecond pulses. Fourth, for 75-ps pulses with no prepulse, the absorptance is insensitive to irradiance in the 2.5×10^{14} to 10^{16} W/cm^2 range.[8] On the other hand, the absorptance did decrease with increasing pulse length (21-ps to 250-ps).[6] Finally, saturation of the backscatter was observed in only one case,[10] indicating that either a prepulse or a longer pulse would lead to increased backscatter and reduced absorption.

Fortunately, several other experiments indicate that neither multinanosecond pulses nor pulses with a leading, low-power-density foot have inherently low absorption at power densities of less than 10^{15} W/cm^2. Ripin[3] has measured an absorptance of > 0.55% for 3-ns, 1.06-μm pulses at power densities of 7×10^{14} W/cm^2, and we[13] have measured an absorptance of 0.7 at 10^{14} W/cm^2 for 8-ns, 1.06-μm pulses. Both of these are higher than the maximum absorptance (~ 0.5) observed with subnanosecond pulses[8,14] at these power densities. Also, the recent experiments of Fabre[11] which used 100-ps pulses indicate that a low-power-density foot on a pulse may not cause the same scattering problems as the distinct prepulse in Ripin's experiments. Although Fabre's results are questionable because of detector sensitivity at his laser intensity and the time between the onset of the prepulse and main pulse, he found that a distinct prepulse increased backscatter whereas a continuous, low-power-density foot did not affect the backscatter. For longer pulses, Mallozzi[12] found that the reflected laser light decreased from about 70% for a 1-ns 10^{11} W/cm^2 foot to nearly 40% for a 10-ns, 10^{11} W/cm^2 foot. Here, and in most other experiments to be discussed, there does not appear to be a simple correlation between short and long pulse experiments. Even though all of the experiments discussed thus far have been for 1.06-μm laser light, no dramatic changes are expected for the near 3-μm HF laser radiation. The backscatter has not been a

problem in the 10.6-μm, CO_2 laser-target experiments at LASL; the maximum backscatter percentage has been less than about 5%.[2] Furthermore, the broadband nature of the HF irradiation should further reduce the stimulated scattering. Collectively, these experiments imply that Brillouin scattering should be independent of the HF pulse shape and should not be an important energy-loss mechanism in the HF laser-target experiments.

IV. Effect of a Prepulse on X-ray Conversion Efficiency

There is only limited data on the x-ray production, high-energy electrons and ions, harmonic emission, and plasma density profiles formed by pulses with some type of prepulse. For single 75-ps pulses, NRL[8] found that as the irradiance increases, the absolute x-ray emission near 1 keV remains almost constant while the higher energy portion of the spectrum increases dramatically. When a distinct prepulse is introduced, increasing η (η = prepulse energy/total incident energy) causes the x-ray emission near 1 keV to increase and the higher energy x-ray emission to decrease. This is interpreted to imply that a prepulse increases the thermal conductivity of the plasma and decreases the hot electron temperature. Fabre[11] also observed these trends. In contrast to the x-ray results, the absolute number of fast electrons has been found to increase for a moderate prepulse level. For a single, 75-ps pulse with an average irradiance of 7×10^{15} W/cm^2, NRL's electron spectrometer data[6] indicates a Maxwellian electron energy distribution with kT_e = 42 keV (for energies > 50 keV). A pulse of the same irradiance but with a prepulse of level η = 0.1 shows a highly non-Maxwellian spectrum with an enhancement of electrons in the 150-200 keV energy range. This enhancement of fast electrons is attributed to an enhanced level of parametric instability heating in the underdense plasma. The energy content of these electrons is insignificant ($\sim 10^{-4}$ of incident energy), and therefore the general trend towards a softer x-ray spectrum is viewed as favorable for laser-fusion applications.

If this same trend occurs for multinanosecond pulses, it would be unfavorable for weapons-effects-simulation. As with the absorptance, it is dangerous to draw any general conclusions from these limited, short-pulse experiments. For example, although Mallozzi did not systematically vary the prepulse, he measured the 4π conversion efficiency to be between 13% and 20% for the conversion of laser energy into x-rays with energy greater than 1 keV. He used a 1-2 ns (FWHM) main pulse with a focal power density between 10^{13} and 2×10^{14} W/cm^2. The prepulse foot varied in length from 1 to 20 ns and had a focused power density of 10^{11} W/cm^2. Mallozzi's conversion efficiency measurements are consistent with measurements of the x-ray conversion efficiency using single 1-ns[15] and 8-ns[16] pulses, which implies that a prepulse foot is unimportant for x-ray conversion efficiencies from multinanosecond, 1.06-μm pulses. In making these comparisons, it is important to note that the x-ray conversion efficiency[17-19] and hot electron temperature[20] increase with laser power density. Also, the x-ray conversion efficiency shows a strong dependence on atomic number.[15,17,18,21] It is, therefore, very difficult to make comparisons.

It is also difficult to draw conclusions about prepulse effects at $\sim 3\mu$m. Richardson[19] has observed a decrease in both line and continuum x-ray emission intensity when energetic prepulses ($\eta \approx .001$) are present in 10.6-μm pulses. However, this reduction due to a prepulse may be small compared to the decrease due to the wavelength effect. Experiments at NRC[19] and LASL[22] both have shown that by going from 1.06-μm to 10.6-μm pulses at $\sim 10^{14}$ W/cm^2, the x-ray conversion efficiency decreases by a factor of 10 to 20. These experiments indicate that it is more important to quantify the x-ray spectrum and conversion efficiency at $\sim$ 3-μm irradiation than it is to be initially concerned with the effect of the prepulse.

V. Numerical Simulations

In general, the experimental results on prepulse effects are incomplete. Extrapolating any of these results to give predictions about the importance of the prepulse level of long, HF pulses is unreasonable, if not impossible. Therefore, we have used our one-dimensional hydrodynamics-heat flow code (CHAMISA) to study the effect of prepulse level in idealized HF laser pulses. For the 8-ns, 1.06μm pulses, this code has accurately predicted the ablation velocities[23] and relative absorptances,[13] and given reasonable estimates of the x-ray conversion efficiencies for low-Z materials.[16] Since our initial HF laser-target experiments will emphasize such measurements as the absorption, x-ray conversion efficiency, x-ray spectrum, and target ablation velocities, CHAMISA should give a good estimate of the importance of the prepulse level. The major weakness is in calculating x-ray emission from high-Z materials. The x-ray energy loss package calculates only losses by free-free and free-bound transitions with hydrogenic approximations. This treatment is totally inadequate for higher Z materials where line radiation, radiation transport, and non-equilibrium processes are important, but difficult, and perhaps impossible to calculate. By ignoring the line radiation for high-Z materials, we underestimate the low energy radiation losses, resulting in an increased plasma temperature. In turn, the average ionization state determined from the equilibrium equation-of-state tables is abnormally high and the radiative recombination is both enhanced (Z^4 dependence from a hydrogenic approximation) and displaced to larger photon energies. This potentiation effect is not a problem for low-Z materials which are nearly fully ionized at the power densities of interest here. Any results for high-Z materials, therefore, should be viewed skeptically. Nevertheless, the relative values of absorptance, x-ray conversion efficiency, and ablation

velocities as a function of prepulse power density should be indicative of experimental trends. With this in mind, we have performed a series of calculations which study the effect of prepulse power density, flux limit, and wavelength on targets of Al and Au.

For all of the simulations, we assume that the main pulse and the prepulse are 5-ns, constant power density pulses. The main pulse was always 10^{14} W/cm^2 and we used three prepulse levels: 10^{12} W/cm^2, which represents a realistic prepulse from the PHOENIX II laser system; 10^{10} W/cm^2, which represents a prepulse which may be realistic after long-term laser development; and no prepulse, which is an idealized case for purposes of comparison. The value of the flux limit parameter was chosen to be 0.6, which represents the classical electron heat flux and is an optimistic estimate of the thermal conductivity, or 0.03, which is a severe flux limit and is a pessimistic estimate of the heat flow. Since ponderomotive forces were not included in the calculations, the 0.03 flux limit can also be viewed as representing the profile steepening caused by ponderomotive forces. No hot electrons were generated or transported. We assumed classical inverse bremsstrahlung absorption in all of the calculations.

In Fig. 1 we illustrate typical velocity (v), electron temperature (T_e), and density (ρ) profiles which are observed in the simulations of Al targets. We chose to show the profiles at 3-ns after the onset of the 10^{14} W/cm^2, constant power density pulse because they illustrate the long pulse stationary flow and ablative behavior. The shape of the v, T_e, and ρ profiles in the region from 80- to 200-μm is observed to be effectively constant after approximately 1-ns from the beginning of the pulse. This behavior is typical of the stationary flow behavior observed for long pulses.[24,25] We also find that these profiles are not significantly affected by the prepulse levels. The v profile illustrates the effect of

stationary flow on the ion exhaust velocity; a large fraction of the mass is accelerated to the same velocity, namely, the ablation velocity. Note also that although the entire plasma at distances greater than about 90 μm is emitting x-rays, the majority of the emission is in the overdense plasma (~ 90-180 μm) inside the critical surface (~280 μm). The increased density in this region more than compensates for the reduced electron temperatures.

In Tables I, II, and III we summarize the results by showing the fraction of laser energy absorbed (absorptance, A), the fraction of the absorbed laser energy which is converted to plasma kinetic (f_K) and x-ray (f_R) energies, the maximum electron temperature (T_e^{max}), the ablation velocity (v_A), and penetration depth of the laser energy (Δx) for the various parameter variations. Each table illustrates the effect of prepulse levels (I_p) at the two values of the electron thermal conduction flux limit (f). A material comparison can be made with Table I and Table II for 3.0-μm irradiation. A comparison of different wavelength irradiance of Al targets can be made with Tables I (3.0-μm) and III (1.06-μm). The prepulse has little effect on any of these laser-target interaction characteristics. That is, for a given material, wavelength, and flux limit, the values of the absorptance, x-ray conversion efficiency, and target ablation are only weakly dependent on the prepulse intensity. This negligible effect indicates that the initial emphasis should be on target experiments with the existing HF pulses rather than on experimental work on prepulse suppression and target isolation.

The x-ray conversion efficiency and x-ray spectrum are of particular interest for the weapons-effects-simulation program. In Table IV we list the fraction of laser energy which is converted into x-rays with energies above 1 keV and 10 keV. The code runs from Tables I, II, and III, with 10^{12} w/cm^2 prepulse used in these calculations. The higher conversion efficiencies for Au targets for 3.0-μm irradiation illustrate the major problem in the calculations. We calculate only

bremsstrahlung and recombination radiation losses and we assume that an ionization equilibrium is established at the local electron temperature. These assumptions lead to a hot, highly stripped plasma in which radiation losses are dominated by radiative recombination. Furthermore, the recombination edge can be as high as 20 keV. For intermediate to high-Z materials, line radiation dominates the continuum radiation and deviations from ionization equilibrium are known to be large.[14,26] Therefore, the conversion efficiencies in Table IV should be viewed only for trends which occur with changes in wavelength, materials, and thermal conductivity. More detailed calculations which include hot electron generation and transport, line emission, and radiation transport are in progress. However, these calculations will require benchmark experiments for parameter normalization.

Another problem is the effect of a preformed plasma on the performance of complex, laser-fusion targets. To estimate the importance of the prepulse on these targets, we compare the ablation velocities as a function of power density, as listed in Table V. To within 50%, the ablation velocities are independent of the flux limit. Furthermore, the ablation velocity is only weakly dependent on power density, varying roughly as the $I^{1/4}$ to $I^{1/2}$ dependences predicted earlier.[25] The time required for the plasma to move some arbitrary distance gives an estimate of the prepulse importance. At 10^{10} W/cm^2, the time for the plasma to travel 100μm is approximately 2 ns, whereas at 10^{14} W/cm^2, the equivalent time is 0.1 ns. Thus for multinanosecond pulses, detrimental effects will be observed very early in the main pulse and the question of prepulse is irrelevant. Of course, for pulses in the neighborhood of a few nanoseconds with good spatial beam quality and an intensity such that ponderomotive forces are dominant, this simple argument does not apply.

VI. Conclusions

In summary, neither previous experiments nor numerical simulations indicate that the prepulse foot on the multiplexed, HF laser pulses will degrade the target performance. For our immediate goals, it is much more important to measure the absorption, x-ray spectrum, x-ray conversion efficiency, and target ablation using the existing pulses than it is to work on eliminating the prepulse. Ultimately, however, results using HF radiation should be compared with results using 1.06 μm and 10.6 μm lasers. The best comparisons would result from eliminating the HF prepulse. Alternatively, a prepulse could be added to the glass or CO_2 lasers. Unless the initial HF target studies dictate otherwise, work in the general area of HF pulse shaping should be a low priority.

References

1. G. C. Tisone (private communication).
2. D. Giovanielli (private communication).
3. NRL Laser Plasma Interaction Group, B.H. Ripin, editor, NRL Memorandum Report 3890, December 1978.
4. Yu. A. Bykovskii, N. N. Degtyarenko, V. F. Elesin, Yu. P. Kozyrev, and S. M. Sil'nov, Soviet Physics JETP 33, 706 (1971); P. E. Dyer, S. A. Ramsden, J. A. Sayers, and M. A. Skipper, J. Phys. D: Appl. Phys. 9, 373 (1976).
5. J. L. Nuckolls, L. Wood, A. Thiessen, and G. Zimmerman, Nature (London) 239, 139 (1972).
6. C. M. Armstrong, B. H. Ripin, F. C. Young, R. Decoste, R. R. Whitlock, and S. E. Bodner, NRL Memorandum Report 3820, August 1978.
7. B. H. Ripin, J. A. Stamper, and E. A. McLean, "Effects of Target Material, Geometry, and Prepulse Timing on the Brillouin Backscatter Instability," presented at the IEEE Conference on Plasma Science, Monterrey, California, May 1978.
8. B. H. Ripin, NRL Memorandum Report 3604, December 1977.
9. B. H. Ripin, F. C. Young, J. A. Stamper, C. M. Armstrong, R. Decoste, E. A. McLean, and S. E. Bodner, Phys. Rev. Lett. 39, 611 (1977).
10. B. H. Ripin, J. M. McMahon, E. A. McLean, W. M. Manheimer, and J. A. Stamper, Phys. Rev. Lett. 33, 634 (1974).
11. F. Amiranoff, R. Benattar, R. Fabbro, E. Fabre, C. Garban, C. Popovics, A. Poquerusse, R. Sigel, C. Stenz, J. Virmont, and M. Weinfeld, "Experimental Studies of Interaction and Transport Processes in Laser Fusion," presented at the 7th International Conference on Plasma Physics and Controlled Nuclear Fusion Research, Innsbruck, Austria, August 1978.

12. P. J. Mallozzi, H. M. Epstein, R. G. Jung, D. C. Applebaum, B. P. Fairand, and W. J. Gallagher, in Fundamental and Applied Laser Physics, edited by M. S. Feld, A. Javan, and N. A. Kurnit (John Wiley and Sons, New York, 1971) pp. 165-220.

13. J. P. Anthes, M. A. Palmer, M. A. Gusinow, and M. K. Matzen, "Absorption of Laser Radiation by Al, Fe, and Au Planar Metallic Targets," accepted for publication in J. Appl. Phys.

14. M. D. Rosen, W. C. Mead, J. J. Thomson, and W. L. Kruer, UCRL-80862, March 1978.

15. J. A. Stamper and L. S. Levine, editors, NRL Report 7838, October 1974, p.93.

16. M. A. Gusinow, D. Woodall, J. P. Anthes, M. A. Palmer, E. J. McGuire, M. K. Matzen, and K. M. Gilbert, SAND78-0920, June 1978.

17. H. Pepin, R. Grek, F. Rheault, and D. J. Nagel, J. Appl. Phys. 48, 3312 (1977).

18. R. D. Bleach and D. J. Nagel, J. Appl. Phys. 49, 3832 (1978).

19. G. D. Enright, N. H. Burnett, and M. C. Richardson, Appl. Phys. Lett. 31, 494 (1977).

20. D. W. Forslund, J. M. Kindel, and K. Lee, Phys. Rev. Lett. 39, 284 (1977).

21. K. M. Gilbert, J. P. Anthes, M. A. Gusinow, M. A. Palmer, D. J. Nagel, and R. R. Whitlock, submitted for publication in J. Appl. Phys.

22. D. J. Nagel (private communication).

23. J. P. Anthes, M. A. Gusinow, and M. K. Matzen, Phys. Rev. Lett. 41, 1300 (1978).

24. S. J. Gitomer, R. L. Morse, and B. S. Newberger, Phys. Fluids 20, 234 (1977).

25. M. K. Matzen and R. L. Morse, "Structure and Observable Characteristics of Laser-Driven Ablation," accepted for publication in Phys. Fluids.

26. M. K. Matzen and J. S Pearlman, "Impact of Nonequilibrium Ionization and Recombination Processes on the Evaluation of Laser-Produced Plasmas," accepted for publication in Phys. Fluids.

Figure Captions

Figure 1. The velocity (v), electron temperature (T_e), and density (ρ) profiles of the Al plasma after 3 ns of 10^{14} W/cm^2, 3.0-μm, constant-power-density irradiation of an Al target. The position of the critical density (N_c) and the region of > 95% of the radiation emission are shown.

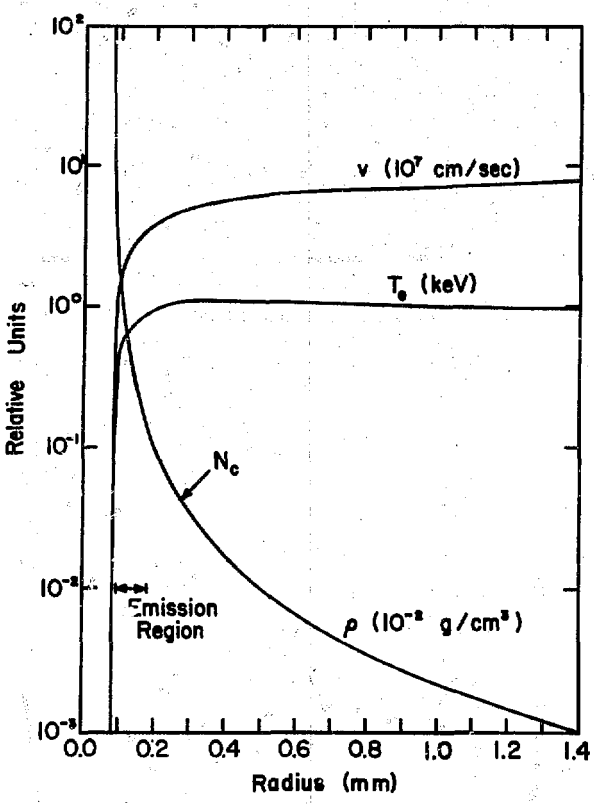
Relative Units
10^{2}
10^{1}
10^{0}
10^{-1}
10^{-2}
10^{-3}
v (10^{7} cm/sec)
T_e (keV)
N_c
Emission Region
ρ (10^{-2} g/cm^3)
0.0
0.2
0.4
0.6
0.8
1.0
1.2
1.4
Radius (mm)

Table I.

The parameters for the plasma produced from an Al target by using a 5 ns. 10^{14} W/cm^2 constant power, 3.0-μm laser pulse with various prepulse power densities (I_p) and electron thermal conduction flux limits (f). The absorptance (A), the fraction of absorbed laser energy converted into plasma kinetic (f_K) and x-ray energy (f_R), the maximum electron temperature (T_e^{max}), the ablation velocity (v_A), and the penetration depth of the laser (Δx) are shown.

I_p	f	A	f_K	f_R	T_e^{max}(keV)	v_A(10^8cm/s)	Δx (μm)
0	0.6	0.65	0.928	0.048	1.1	0.84	2.39
10^{10}	0.6	0.65	0.928	0.046	1.1	0.84	2.48
10^{12}	0.6	0.63	0.929	0.046	1.2	0.86	2.44
0	0.03	0.16	0.969	0.019	2.0	1.06	0.44
10^{10}	0.03	0.16	0.953	0.028	2.0	1.02	0.58
10^{12}	0.03	0.14	0.962	0.020	2.3	1.06	0.48

Table II

The plasma parameters produced by a 5 ns, 10^{14} W/cm^2 constant power, 3.0-μm laser pulse on Au targets. The prepulse levels, flux limits, and symbols are the same as in Table I.

I_p	f	A	f_K	f_R	T_e^{max}(keV)	$v_A(10^8$cm/s)	Δx(μm)
0	0.6	0.83	0.685	0.301	1.8	~ 1.0	0.24
10^{10}	0.6	0.84	0.681	0.303	1.8	~ 1.0	0.25
10^{12}	0.6	0.83	0.687	0.294	1.8	~ 1.0	0.26
0	0.03	0.33	0.944	0.041	~ 4	~ 1.3	0.078
10^{10}	0.03	0.31	0.937	0.044	~ 4	~ 1.3	0.087
10^{12}	0.03	0.32	0.930	0.047	~ 4	~ 1.3	0.10

Table III

The plasma parameters produced by a 5 ns, 10^{14} W/cm^2 constant power, 1.06-μm laser pulse on Al targets. The prepulse levels, flux limits, and symbols are the same as in Table I.

I_P	f	A	f_K	f_R	T_e^{max}(keV)	$v_A(10^8$cm/s)	$\Delta x(\mu m)$
0	0.6	0.95	0.911	0.068	1.2	0.84	3.8
10^{10}	0.6	0.95	0.909	0.069	1.2	0.84	3.9
10^{12}	0.6	0.95	0.908	0.069	1.2	0.86	4.0
0	0.03	0.55	0.940	0.048	~2.3	1.07	1.6
10^{10}	0.03	0.52	0.939	0.048	~2.0	1.07	1.6
10^{12}	0.03	0.54	0.934	0.049	~2.0	1.06	1.8

Table IV

The fraction of the incident laser energy which is converted into x-rays with energies above 1 keV and 10 keV is shown as a function of material, wavelength (λ) and flux limit (f). All laser pulses consisted of a 5 ns, 10^{12} W/cm^2 foot preceding a 5 ns, 10^{14} W/cm^2 main pulse.

Material	λ (μm)	f	F > 1 keV	F > 10 keV
Al	3.0	0.6	.014	4.2×10^{-7}
Al	3.0	0.03	.0012	3.2×10^{-7}
Au	3.0	0.6	.060	7.7×10^{-3}
Au	3.0	0.03	.010	1.0×10^{-3}
Al	1.06	0.6	.031	2.0×10^{-6}
Al	1.06	0.03	.013	7.1×10^{-6}

Tabla V

The ablation velocity as a function of flux limit (f) and power density (I) for 3.0-μm irradiation of Au targets.

$I(W/cm^2)$	v(cm/s)	
	f=0.6	f=0.03
10^{10}	$\sim 3 \times 10^6$	$\sim 5 \times 10^6$
10^{12}	2.5×10^7	4×10^7
10^{14}	$\sim 10^8$	$\sim 1.5 \times 10^8$

Distribution:

4000 A. Narath
4200 G. Yonas
4210 J. B. Gerardo (2)
4211 E. J. McGuire
4211 M. K. Matzen (15)
4212 R. A. Gerber
4212 G. A. Fisk
4212 A. K. Hays
4212 G. N. Hays
4212 J. M. Hoffman
4212 J. B. Moreno
4212 T. D. Padrick
4212 H. L. Patterson
4212 J. K. Rice
4212 G. C. Tisone
4212 W. M. Trott
4212 F. K. Truby
4212 J. R. Woodworth
4214 E. D. Jones
4216 A. W. Johnson
4230 M. Cowan, Jr.
4234 R. E. Palmer
4234 J. P. Anthes
4234 M. A. Palmer
8266 E. A. Aas
3141 T. L. Werner (5)
3151 W. L. Garner (3)
For: DOE/TIC (Unlimited Release)
DOE/TIC
3154-3 R. P. Campbell (25)